Published by The College of Science & Information Technology (COSIT), TASUED, Vol. 19, No. 1, pp. 1-9.

COSIT, TASUED
Journal of Science and Information Technology (JOSIT)

Investigation of Horizontal Magnetic Field (SYM-H) using Non-Linear Time-Series and Wavelet Analysis

[1]Bamidele, K. J.; [2]Kotoye, A. A.; [1]Adelaja, A. D.; [1]Fowodu., T. O.; [1]Fagbohun, M. A.; [1]Oloyede, E. S.; [1]Falayi, E. O.

[1]Department of Physics, Tai Solarin University of Education, Ijagun, P.M.B. 2118 Ijebu-Ode, Ogun State, Nigeria
[2]Department of Science Laboratory Technology, Abraham Adesanya Polytechnic, Ijebu Igbo, Ogun State, Nigeria
Corresponding Author: bamidelekj@tasued.edu.ng

Abstract

The horizontal geomagnetic field (SYM-H) is a geomagnetic field parameter for measuring the severity of geomagnetic storm. We investigated SYM-H using nonlinear time series and Wavelet power spectrum using a high resolution data of 1-minute obtained from the Flight Center Space Physics Data Facility (GSFC/SPDF) OMNIWEB interface spanning from 1st January to 31st December, 2014. Wavelet power spectrum (WPS) analysis assists in breaking down the time series of SYM-H s into different scales. The results revealed that the months of January, August and October displayed more enhancement of geomagnetic storms. The nonlinear time series modelling was also applied to study SYM-H using both the time delay and embedded dimension in computing average mutual information (AMI) and false nearest neighbours (FNN), respectively. The Lyapunov exponent (LE) was computed using the results obtained from AMI and FNN. The results revealed that LE displays positive values, indicating that SYM-H is a deterministic chaotic system.

Keywords: Horizontal Magnetic Field, Lyapunov Exponent, Wavelet Power Spectrum, Nonlinear Time Series, Embedded Dimension.

INTRODUCTION

The horizontal geomagnetic field (SYM-H) measures the severity of the geomagnetic storm disturbance of the Earth's magnetic field (Falayi et al., 2020). Geomagnetic storms are well observed phenomena that enhance the plasma of the inner magnetosphere to high energies. When the solar wind and the geomagnetic field interact, it results in the magnetospheric activity, which is measured by the global magnetospheric indices and includes auroras, turbulence, ionospheric currents, magnetic reconnection, and geomagnetic storms. In order to fully understand the dynamics of natural time series, this study employs numerical tools such as wavelet transform and nonlinear techniques. Wavelet transform is utilized to simultaneously break down a one-dimensional signal into two-dimensional temporal frequency domains to examine localized fluctuations within a time series (Riabova, 2018; Adamowski et al., 2009). Deterministic components in the data are differentiated from other stochastic components applying nonlinear (chaotic) techniques. There are numerous applications of the wavelet transform in geophysics and space physics for example (Riabova, 2018; Gao and Yan, 2011; Falayi *et. al*. 2018; Bremaud, 2014; Arneodo *et. al.*, 1991; Han and Chang 2013; Falayi *et al*. 2020). The idea of wavelet is applied to ionospheric and magnetospheric studies of atmospheric cold fronts (Meyers and Kelly, 1993), in coherent strutures in turbulent flows (Farge, 1992).

Chaos has also been applied widely in several related fields, notably weather and climate forecasting (Fuwape *et al.* 2016; Ogunsua *et al*. 2014; Rabiu *et al*. 2014;

Cite as:

Bamidele, K.J.; Kotoye, A.A.; Adelaja, A.D.; Fowodu., T.O.; Fagbohun, M.A.; Oloyede, E.S.; Falayi, E.O. (2025). Investigation of Horizontal Magnetic Field (SMY–H) using Non-Linear Time-Series and Wavelet Analysis. *Journal of Science and Information Technology (JOSIT)*, Vol. 19, No. 1, pp. 1-9.

Unnikrishnan and Ravindran, 2010). Falayi *et al*. applied Chaos in 2020 to investigate the geomagnetic field's parameters for one solar cycle. In this research, horizontal geomagnetic horizontal geomagnetic field (SYM-H) from January 1st – December 31st, 2014 was studied using wavelet analysis and nonlinear time series.

MATERIALS AND METHODS

Here, we analyzed horizontal geomagnetic field (SYM-H). The 1-minutes resolution data used were obtained from the Flight Center Space Physics Data Facility (GSFC/SPDF) OmniWeb (http://omniweb. gsfc.nasa.gov) interface between January 1st – December 31st, 2014. The year is considered as a year of solar maximum.

Wavelet power spectrum analysis (WPS)

A technique to obtain the frequency of occurrences in relation to their location within a time series is the wavelet power spectrum. Equation (1) reveals the non-analytic Morlet wavelet, a function defined by a single parameter, was employed for obtaining the results that were presented.

$$\psi_{a,b(t)} = a^{1/2}\psi(\frac{t-b}{a}) \quad (1)$$

where:
a represents the scale associated with the wavelet's increase and decrease.
b symbolises the time localization.

Morlet wavelet is obtained in equation (2) as (Torrence and Compo, 1998):

$$\psi_{(t)} = \frac{e^{i\omega_o t}}{\sqrt[4]{\pi e^{\frac{t^2}{2}}}} \quad (2)$$

where, ω_o is the non – dimensional frequency parameter of equation (2) (Riabova, 2018; Falayi et. al., 2020; Kumar and Foufoula – Georgia ,1997)

The time series of the data of Morlet wavelet is presented in equation (3) (Falayi et. al., 2020; Kumar and Foufoula–Georgia, 1997).

$$wps_{(a,b)} = \int_{-\infty}^{\infty} x(t)\psi^* a,b\,(t)dt \quad (3)$$

where, $\psi_{a,b}{}^*(t)$ denoted as the conjugate of wavelet function $\psi_{a,b}(t)$. The expression of the wavelet coefficient at time index n and scale a is expressed in equation (4):

$$wps_n(a) = \sum_{n'=0}^{N-1} x((n')\psi^* \left[\frac{(n'-n)dt}{a}\right] \quad (4)$$

Figures 1(a)–(c) show the wavelet power spectrum analysis to estimate the time-frequency characteristic of the SYM–H between January 1st – December 31st, 2014.

Nonlinear dynamical techniques

We analyzed the Lyapunov exponent, average mutual information (AMI), and false nearest neighbor (FNN) in order to investigate the chaotic time series of SYM-H. To obtain the dynamical properties of a system, the SYM-H time series data requires space phase reconstruction with embedding dimension (m) and time delay (s) (Takens, 1981). Equation (5) is used to generate this.

$$P(t) = \left(M_t, M_{t-\tau}, M_{t-2\tau.....}M_{t-(x-1)\tau}\right) \quad (5)$$

where x and τ suggests the embedding dimension and time delay, correspondingly.

The phase reconstructions of SYM-H may be determined from the initial minimum values of AMI were chosen as the delay time (Shaw, 1981; Fraser and Swinney, 1986; Kennel et al., 1992). The AMI technique is predictable by Equation (6):

$$Q = -\sum I_{kl(\tau)} \ln \frac{I_{kl}(\tau)}{I_{kl}} \quad (6)$$

where k and $I_{kl}(\tau)$ are the combined probabilities that a time series value can be obtained in segment k at time t and l at time t + τ. I_k is the likelihood of finding a time series value in the interval. For various locations, the initial lowest value of Q is regarded as the time delay (τ). The Fig 2(a)–(c) show the average mutual information AMI for SYM–H between January 1st – December 31st, 2014.

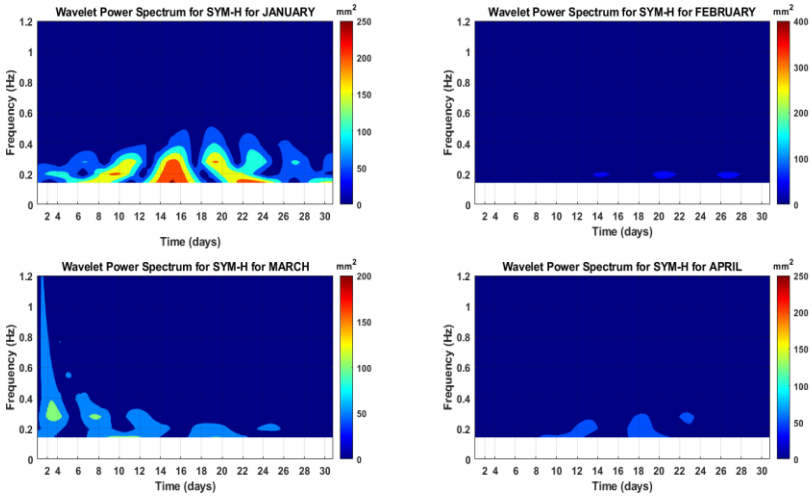

(a)

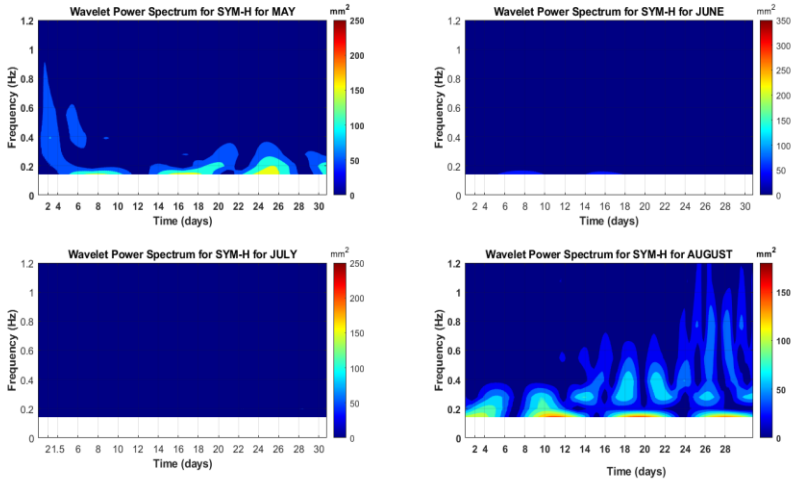

(b)

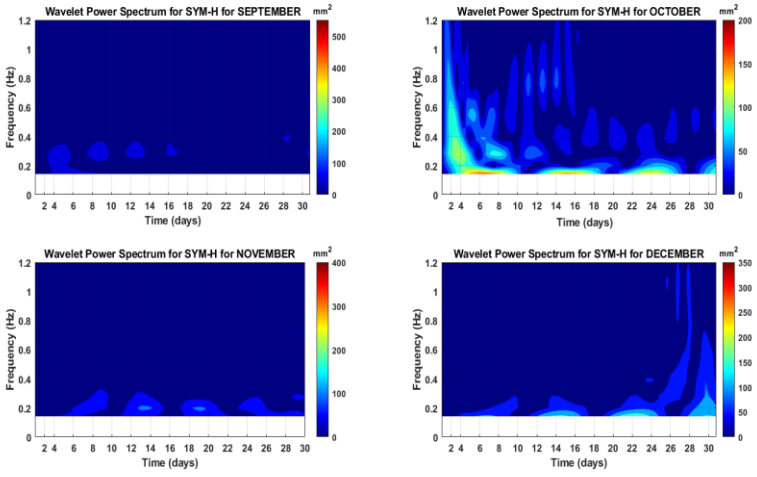

(c)

Figures 1. Depict the wavelet power spectrum for SYM–H between January 1st – December 31st, 2014.

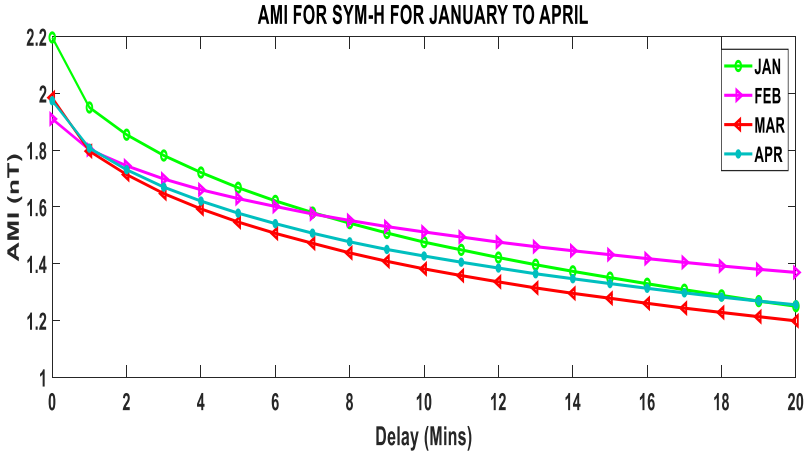

(a)

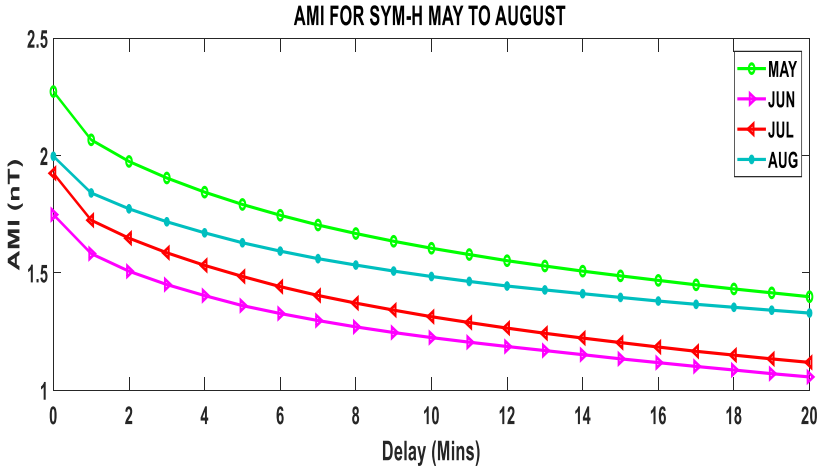

(b)

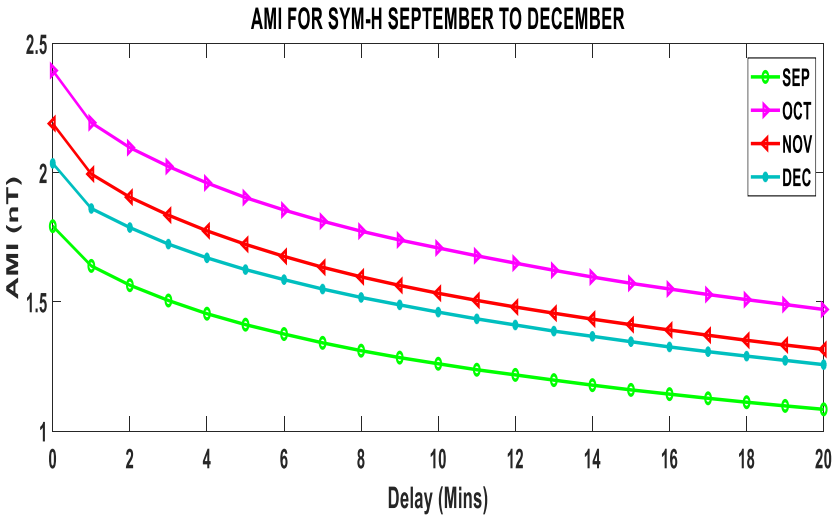

(c)

Figure 2. Average mutual information AMI of SYM-H from 1st January to 31st December, 2014.

In order to identify the embedding dimension and eliminate the unfitting neighbours, nonlinear systems' dynamics can be clarified or rebuilt using the false nearest neighbours (FNN). FNN varies as the embedding dimension intensifies along the path. Because of prediction, the points in a dimension are near to one another; this will be divided in upper dimensions. When advancing from d to d +1, the difference between two relative distance neighbour points strengthens and serves as a degree for casting embedding mistakes. The technique utilized by Falayi *et al*. (2020), Ogunsua *et al*, (2014) and Kennel et al. (1992) was applied to determine the embedding dimension of SYM-H. Equation (7) provides the expression for the false nearest neighbour distance.

$$\left[\frac{X^2_{d+1}(t,r)-X^2_d(t,r)}{X^2_d}\right]^{\frac{1}{2}}=\left[\frac{y(t+r)-y(t_\tau+\tau)}{X_d}\right]\succ X_{tot} \quad (7)$$

where neighbour and origin points are denoted by the letters t and t_r, respectively. (see Figure 3a-c)

Lyapunov Exponent

The Lyapunov exponent is chaotic quantifier. The LE is used to explain when the near trajectories diverge or converge in one dimension. A positive Lyapunov exponent indicates that there is evidence of chaos in a dissipative deterministic system, where the positive Lyapunov exponent indicates divergence of trajectory (Falayi et al., 2020; Ogunsua et al., 2014; Eckman and Ruelle 1985). The huge Lyapunov exponent (λ) can be used to determine the rate of divergence as obtained by (Abarbanel and Lali 1996) using equation 8.

$$\lambda=\lim\frac{1}{n}\ln\frac{\left|\Delta x(\boldsymbol{X}_o,n)\right|}{\left|\Delta \boldsymbol{X}_o\right|} \quad (8)$$

where λ represent Lyapunov exponents (LE) and it is applied for differentiating different kinds of paths and to determine the rate of divergence.

The exact estimation of a chaotic dynamical structure is a component of the major Lyapunov exponent (Abarbanel and Lali 1996) which is expressed using Equation (9).

$$\Delta_n=\frac{1}{\lambda_{\max}} \quad (9)$$

The Lyapunov exponent was computed for the SYM-H values from January to December. The choice of embedding dimension τ = 25 and delay m = 5 was used for the computed Lyapunov exponent the values of SYM-H were obtained from January to December as shown in Figure 4(a-c).

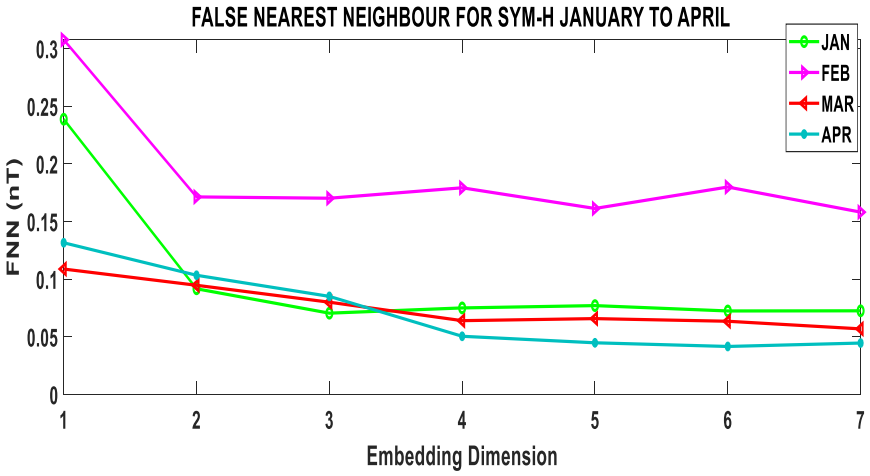

(a)

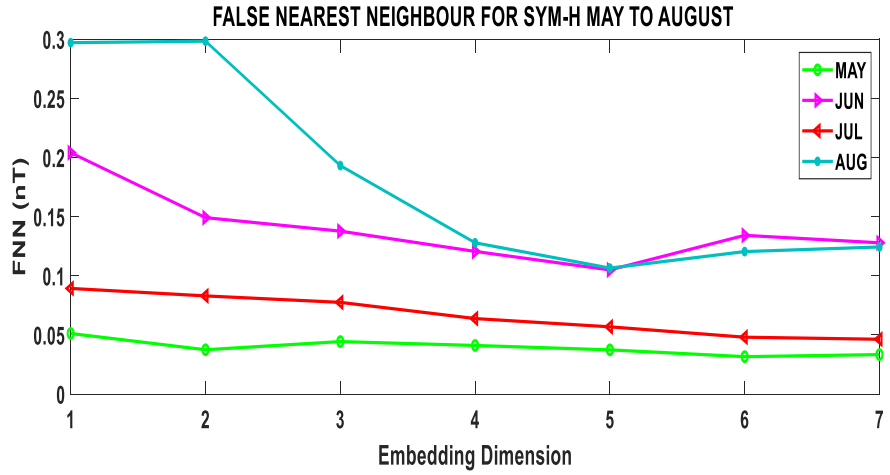

(b)

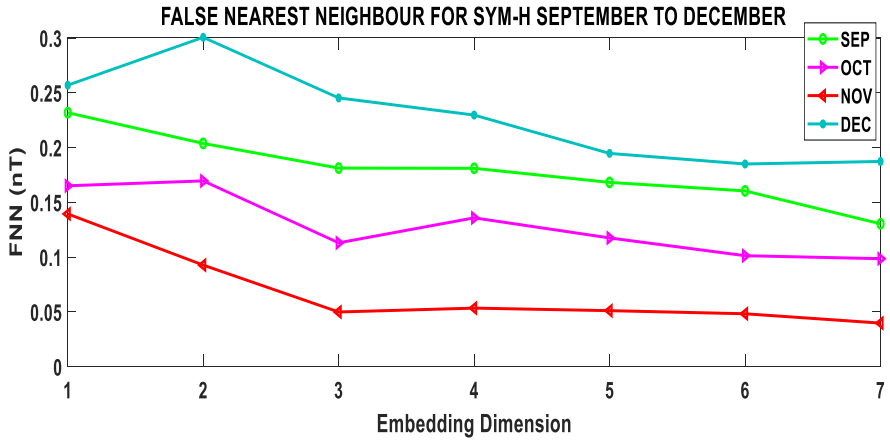

(c)

Figure 3. False Nearest Neighbour FNN of SYM-H from 1st January to 31st December, 2014.

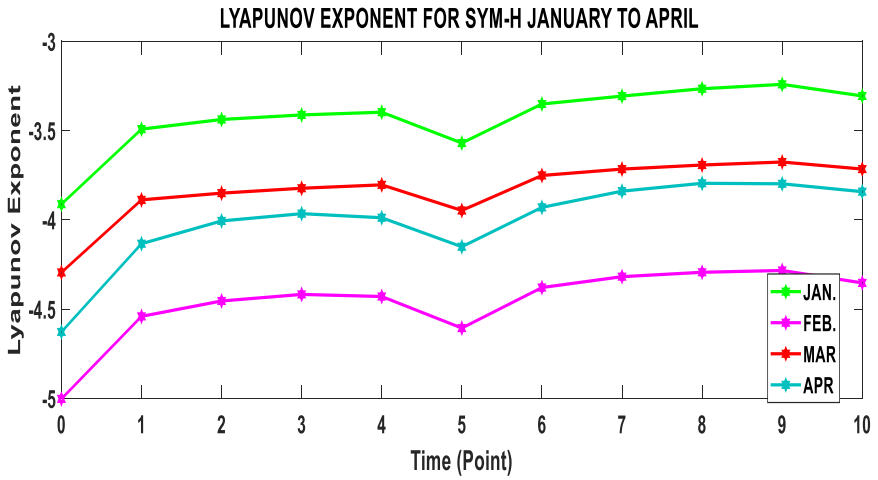

(a)

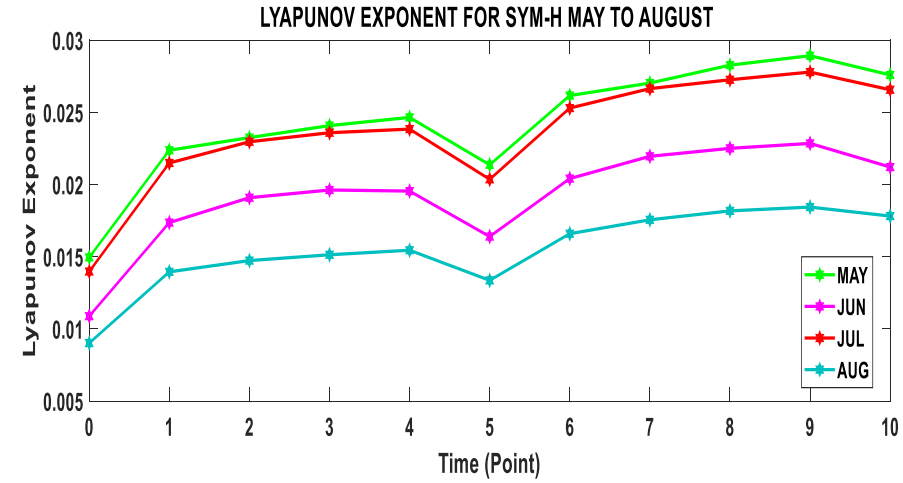

(b)

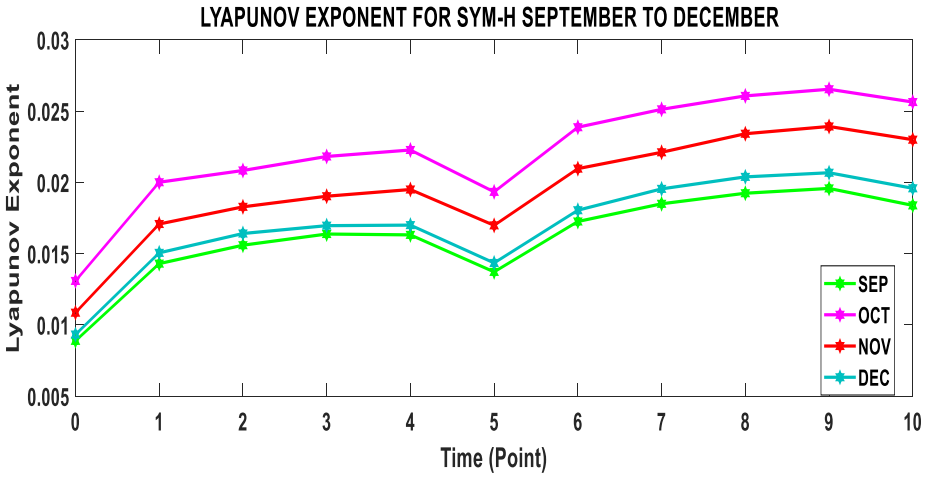

(c)

Figure 4. Lyapunov exponent of SYM-H from 1st January to 31st December, 2014.

DISCUSSION OF FINDINGS

This section presents the results of wavelet power spectrum and Lyapunov exponent from 1st of January to 31st December, 2014 for the horizontal magnetic field (SYM-H).

The wavelet power spectrum was used to decompose the SYM-H into different scales. The results provide more insight on how these variations have changed in frequency and time mode over time. In order to identify SYM-H disturbance storms in time series, the WPS analyses the nonstationary signal. Figures 1(a –c) reveal the power of the WPS for SYM-H from 1st January to 31st December, 2014. The figures also present the real fluctuation of the wavelets character relative to their magnitude. Red depicts the signal's peak energy across the period, while blue denotes a signal with a lower level of intensity. Figure 1a shows the geomagnetic storm is more significant in the month of January, it is severe in the mid of the month and towards the end of month of January while February, March and April display little enhancement of the geomagnetic storm.

The result presented in the Figure 1b show that the months of May and August display more enhancement of the geomagnetic storms compare to the months of June and July, this is strong indicator of change of weather conditions, the month of August demonstrated more enhancement it occurred from the beginning of the month and toward the end of the month of

August the dominant can also be attributed to sudden break of annual rainfall and humidity level.

Figure 1c displayed the variation of the intensity of geomagnetic storm for the months of September, October, November and December using WPS. It was noted that the month of October that the activity of geomagnetic storms is more dominant in the month compared to the other months. The results presented revealed that there is no stable structure during each month from January to December. The frequency of each moths varies (see Figures 1(a-c). It can be noticed that SYM-H showed that variability of the geomagnetic storm. Despite the low solar activity, wavelet coefficients show low power spectrum energy. In contrast to solar maximum conditions, geomagnetic storms are common during the decline phase of the solar cycle and are often minor in magnitude. Falayi et al. (2020) revealed that these storms are connected by streams of high solar wind speed emerging from coronal holes.

The nonlinear behaviour of SYM-H were investigated, the figures 2(a –c) presented show the average mutual information AMI of SYM-H from 1st January to 31st December, 2014. The AMI was computed in order to obtain the time delay function (τ). However, since the AMI and FNN techniques provide an understanding of the complexity of the dynamical system. The Figures 3(a-c) revealed the false nearest neighbour (FNN), the embedding dimension (m) was obtained from a geometrical analysis described as false nearest neighbour (FNN). It is obvious from the Figures 3 (a-c) that the FNN decreases considerably and the least value of (m) relating to the least number of FNN can be measured as the initial information for the selection of embedding dimension. When the false nearest neighbours move towards zero, the preferred dimension is attained. For the months of January, February, March, April, May, June, July, August, September, October, November and December the minimum Embedding dimension (m) appears to be 5 for the SYM-H (see Figures 3 (a-c). The choice of embedding dimension τ = 25 and delay m = 5 was used for the computed Lyapunov exponent presented in Figures 4(a-c) from January to December, 2014. The results exhibit positive Lyapunov exponential values through the year which is the strong indicator of chaos. The values of the Lyapunov exponent range between 0.2632 - 0.1281 from January to December. The month of January displayed high value of Lyapunov exponent compared to the others months while low value was obtained in the month of February.

The results obtained show that the geomagnetic storm is suspected to be a linear system despite that the system producing it (magnetosphere) exhibit nonlinear characteristics (Falayi et al 2021). The erratic behaviour of the magnetosphere could arise from the combined effects of solar wind and internal magnetospheric activity (Unnikrishnan, 2008) similarly, the variations in the magnetosphere-ionosphere system from the solar wind exerts a significant influence on Earth's magnetosphere, which exhibits nonlinear structural extension the magnetosphere system displays internal variability that can be subdued, potentially leading the system toward stochasticity rather than deterministic chaos. Solar winds, acting as stochastic drivers, can induce storms within the system, particularly when coronal mass ejections (CMEs) occur, resulting in geomagnetic storms. The complexity of the ionosphere, as highlighted in previous studies (Bamidele et al., 2025; Falayi et al., 2020; Ogunsua et al., 2014; Unnikrishann and Ravidran, 2010), suggests that the chaotic dynamics resulting from the exponential growth rate of infinitesimal perturbations in the ionosphere may account for the observed variations in Lyapunov exponent values.

CONCLUSION

The study showed the results of the SYM-H using both wavelet spectrum analysis and nonlinear dynamic time series techniques. The enhancement of the geomagnetic storms is more significant in the months of January, August and October, this event can be attributed to coronal mass ejections for the period of high solar activity. The results of the nonlinear dynamic have shown that chaotic features evidently exist in the SYM-H data from the positive Lyapunov exponent from 1st January to 31st December.

REFERENCES

Bamidele, K.J., Adelaja, A.D., Fowodu, T.O., Kotoye, A.A., Ajose, A.S., Falayi, F.C., Falayi., E.O. (2025). Quantitative Analysis of Geomagnetic Indices Using Wavelet Power Spectrum. *Nigerian Journal of Environmental Sciences and Technology*, 9(1), pp. 86-104. https://doi.org/10.36263/nijest.2025.01.14.

Eckman J.P., Ruelle D. (1985). Ergodic theory of chaos and strange attractors. Rev Mod Phys. 57:617–628.

Falayi, E.O., Adewole, A.T., Adelaja, A.D., Ogundile, A.A. & Roy-Layinde, T.O. (2020). Study of nonlinear time series and wavelet power spectrum analysis using solar wind parameters and geomagnetic indices. Nriag Journal of Astronomy and Geophysics. 9(1), 226–237. https://doi.org/10.1080/20909977.2020.1728866.

Falayi, E.O., Ogundile, O.O., Adepitan, J.O., Okusanya, A.A. 2018. Solar quiet variation of the horizontal and vertical components of geomagnetic field using wavelet analysis. Can J Phys. 2018 2034. doi:10.1139/cjp

Foufoula-Georgiou E, Kumar P 1994 Wavelets in geophysics 4 (San Diego: Academic Press)

Fuwape I.A., Ogunjo, S.T., Oluyamo, S.S., Rabiu, A,B. 2016. Spatial variation of deterministic chaos in mean daily temperature and rainfall over Nigeria. Theor Appl Climatol. doi:10.1007/s00704-016-1867-x

Gao R X, Yan R 2011 Wavelets Theory and Applications for Manufacturing (Berlin: Springer)

Han X.H. and Chang X.M. 2013. An intelligent noise reduction method for chaotic signals based on genetic algorithms and lifting wavelet transforms. Inf Sci (Ny). 218:103–118.

Kennel MB, Brown R, Abarbanel HDI. 1992. Determining embedding dimension for phase space reconstruction using a geometrical construction. Phys Rev. 45:3403–3411.

Kumar P, Foufoula-Georgiou E. 1997. Wavelet analysis for geophysical applications. Rev Geophys. 35(4): 285–412.

Ogunsua B.O., Laoye, J.A., Fuwape, I.A., Rabiu, A.B. 2014. The comparative study of chaoticity and dynamical complexity of the low-latitude ionosphere, over Nigeria, during quiet and disturbed days. Nonlin Process Geophys. 21:127–142.

Rabiu AB, Ogunsua B.O., Fuwape I.A., Laoye J.A. 2014. The comparative study of chaoticity and dynamical complexity of the low-latitude ionosphere, over Nigeria, during quiet and disturbed days. Nonlin Processes Geophys. 21:127–142.

Riabova, S. (2018). Application of wavelet analysis to the analysis of geomagnetic field variations. International Conference on Mathematical Modelling in Physical Sciences. IOP Conf. Series: Journal of Physics: Conf. Series 1141 (2018) 012146. doi:10.1088/1742 6596/1141/1/012146

Takens, F (1981).: Detecting Strange Attractors in Turbulence in Dynamical Systems, in: Dynamical systems and Turbulence, Warwick 1980. Lecture Notes in mathematics, Rand, D. and Young, L. S., Springer, Berlin, Heidelberg, vol. 898, https://doi.org/10.1007/BFb0091924, 1981.

Torrence C, Compo GP. 1998. A practical guide to wavelet analysis. Bull Amer Meteor Soc. 79(1):61–78.

Unnikrishnan K, Ravindran S. 2010. A study on chaotic behaviour of equatorial/low latitude ionosphere over Indian subcontinent, using GPS-TEC time series. J Atmos Sol Terr Phy. 72:1080 1089.

Unnikrishnan K. 2008. Comparison of chaotic aspects of magnetosphere under various physical conditions using ae index time series, ann. Geophys. 26:941–953. doi: 10.5194/angeo-26-941-2008.